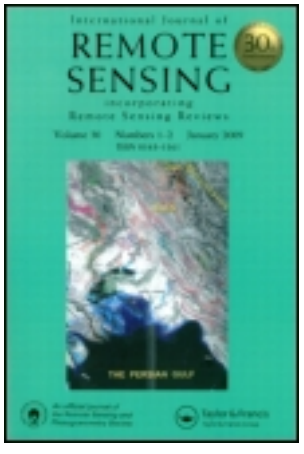

International Journal of Remote Sensing
Publication details, including instructions for authors and subscription information:
http://www.tandfonline.com/loi/tres20

A method for estimating the gross primary production of alpine meadows using MODIS and climate data in China

Fei Li[ab], Xufeng Wang[c], Jun Zhao[d], Xiaoqiang Zhang[e] & Qianjun Zhao[a]

[a] Institute of Remote Sensing and Digital EarthChinese Academy of Sciences, , Beijing, 100101, China

[b] University of Chinese Academy of Sciences, Beijing, 100049, China

[c] Cold and Arid Regions Remote Sensing Observation System Experiment Station, Cold and Arid Regions Environmental and Engineering Research InstituteChinese Academy of Sciences, , Lanzhou, 730000, China

[d] College of Geography and Environmental Science, Northwest Normal University, Lanzhou, 730070, China

[e] Department of Earth and Environmental Sciences, Graduate School and Environmental Studies, Nagoya University, Nagoya, 464-8602, Japan

To cite this article: Fei Li, Xufeng Wang, Jun Zhao, Xiaoqiang Zhang & Qianjun Zhao (2013) A method for estimating the gross primary production of alpine meadows using MODIS and climate data in China, International Journal of Remote Sensing, 34:23, 8266-8286

To link to this article: http://dx.doi.org/10.1080/01431161.2013.834394

International Journal of Remote Sensing, 2013
Vol. 34, No. 23, 8266–8286, http://dx.doi.org/10.1080/01431161.2013.834394

A method for estimating the gross primary production of alpine meadows using MODIS and climate data in China

Fei Li[a,b]*, Xufeng Wang[c], Jun Zhao[d], Xiaoqiang Zhang[e], and Qianjun Zhao[a]

[a]*Institute of Remote Sensing and Digital Earth, Chinese Academy of Sciences, Beijing 100101, China;* [b]*University of Chinese Academy of Sciences, Beijing 100049, China;* [c]*Cold and Arid Regions Remote Sensing Observation System Experiment Station, Cold and Arid Regions Environmental and Engineering Research Institute, Chinese Academy of Sciences, Lanzhou 730000, China;* [d]*College of Geography and Environmental Science, Northwest Normal University, Lanzhou 730070, China;* [e]*Department of Earth and Environmental Sciences, Graduate School and Environmental Studies, Nagoya University, Nagoya 464-8602, Japan*

(*Received 12 October 2012; accepted 2 May 2013*)

The use of remotely sensed data to estimate and monitor the gross primary production (GPP) of an ecosystem on regional scales is an important method in climate change research. Under the unremitting efforts of scientists, many successful remote-sensing-based GPP models have been developed for various vegetation types and regions. However, in practice, some models have been applied to a wide variety of ecosystems, and the suitability of a particular model for the environment under consideration has seldom been taken into account. Due to ecosystem diversity and climatic and environmental variation, it is often difficult to find a model that is suitable for a specific vegetation region. In this article, a new method is proposed for estimating the GPP of alpine vegetation, known as the alpine vegetation model (AVM). The accuracy of the AVM in estimating the GPP was compared to that of four other models: the vegetation photosynthesis model (VPM), eddy covariance–light use efficiency (EC–LUE) model, temperature and greenness (TG) model, and vegetation index (VI) model. The results demonstrated that the AVM displays superior accuracy in estimating the GPP of alpine vegetation. We also found that there is information redundancy in the input variables of these four models, which may account for their lower accuracy in estimating the GPP. In addition, the GPP estimates using the enhanced vegetation index are affected more in the case of low rather than high GPP by the influence of senesced grass during the early and late grassland growing season.

1. Introduction

The global estimation and monitoring of plant photosynthesis (known as gross primary production (GPP)) is a critical component of climate change research (Hilker et al. 2008). Satellite remote sensing provides consistent and systematic observations of vegetation and ecosystems and has played an increasing role in the estimation of GPP (Xiao, Hollinger, et al. 2004). The modelling of carbon cycling requires a parameterization of the land surface (Hall, Townshend, and Engman 1995), which is only possible on a regular basis and in a spatially continuous mode using remote sensing. In the current literature, there are two main barriers to understanding global carbon cycling.

*Corresponding author. Email: lfgis@163.com

Table 1. The remote-sensing-based models used for GPP estimation.

Model	Model structure	Target of model	References
GLO-PEM	$GPP = \varepsilon_0 \times (fPAR(NDVI)) \times (PAR) \times f(T) \times (SM) \times (VPD)$	A variety of ecosystems	Prince and Goward (1995)
3-PG	$GPP = \varepsilon_{\perp 0} \times (fPAR(LAI)) \times (PAR) \times f(T) \times (SM) \times (VPD)$	Forests	Landsberg and Waring (1997)
MODIS-PSN	$GPP = \varepsilon_0 \times (fPAR(NDVI)) \times (PAR) \times f(T) \times (VPD)$	A variety of ecosystems	Running et al. (2000)
C-Fix	$GPP = p(T_{atm}) \times CO_{2\_}fert \times \varepsilon \times (fPAR(NDVI)) \times (PAR)$	Forests	Veroustraete, Sabbe, and Eerens (2002)
VPM	$GPP = \varepsilon_{\perp 0} \times (EVI) \times (PAR) \times f(T) \times f(W)$	Forests	Xiao, Hollinger, et al. (2004) and Xiao, Zhang, et al. (2004)
EC-LUE	$GPP = \varepsilon_0 \times \min\{f(T), f(W)\} \times (fPAR(NDVI)) \times (PAR)$	A variety of ecosystems	Yuan et al. (2007)
TG	$GPP = m \times (scaledEVI) \times (scaledLST)$	A variety of ecosystems	Sims et al. (2008)
VI	$GPP = m \times (EVI)^2 \times (PAR)$	Crops	Wu, Han, et al. (2010) and Wu, Munger, et al. (2010)
AVM	$GPP = m \times (EVI)_{scaled} \times T_{scaled}$	Alpine vegetation	This study (2013)

Note: GPP is gross primary production; ε_0 is apparent quantum yield or maximum light use efficiency; fPAR is the fraction of absorbed photosynthetically active radiation; PAR is the photosynthetically active radiation; $f(T)$ and T_{scaled} refer to the two forms of the temperature stress factor; SM is soil moisture; VPD is water vapour pressure deficit; $f(W)$ is canopy water content; $p(T_{atm})$ is the temperature dependency factor; CO_{2_fert} is the normalized CO_2 fertilization factor; ε is radiation use efficiency; EVI is the enhanced vegetation index; m is a conversion coefficient; the scaledEVI is the difference between EVI and 0.1; and $(EVI)_{scaled}$ is the difference between EVI and EVI_{base}, which is the mean value of EVI over time when the temperature is below 0°C (the biological temperature).

First, high-accuracy models are required. Although there are many remote-sensing-based models available, such as the global production efficiency model (GLO-PEM) (Prince and Goward 1995), Monteith-type parametric model (C-FIX) (Veroustraete, Sabbe, and Eerens 2002), vegetation photosynthesis model (VPM) (Xiao, Hollinger, et al. 2004; Xiao, Zhang, et al. 2004; Xiao et al. 2005), eddy covariance–light use efficiency (EC–LUE) model (Yuan et al. 2007), temperature and greenness (TG) model (Sims et al. 2008), and vegetation index (VI) model (Wu, Munger, et al. 2010) (see Table 1), these models are only applicable to specific areas or sites. There is a need for these models to be investigated in a variety of environments, especially those characterized by climatic conditions and vegetation different from those of the models' target environments.

Second, more field observations are needed to develop and validate remote-sensing-based models. In recent years, a number of field studies have used eddy covariance (EC) techniques, which can provide information on the seasonal dynamics and inter-annual variation of the net ecosystem exchange (NEE), ecosystem respiration (ER), and GPP for studying the carbon cycle in typical forest, grassland, and cropland ecosystems throughout the world (Goulden et al. 1996a, 1996b; Hollinger et al. 1999; Schulze et al. 1999; Law et al. 2000; Yu, Fu, et al. 2006; Yu, Wen, et al. 2006; Yu et al. 2008; Xiao et al. 2008, 2010; Wu, Han, et al. 2010; Wu, Munger, et al. 2010; Wu et al. 2012). In particular, the establishment of the global FLUXNET network provides favourable conditions for studies of the global carbon cycle (http://www.fluxnet.ornl.gov/fluxnet/index.cfm). Continuous network-based observations of the carbon dioxide (CO_2) and energy fluxes over diverse ecosystems can provide integrated information on the ecological processes on ecosystem and regional scales; such valuable data sets (Fu et al. 2010) have enabled the development and validation

of remote-sensing-based models of the carbon exchange between the terrestrial biosphere and the atmosphere.

Consequently, this article is focused on the following three problems: (1) estimating the GPP of alpine vegetation (alpine meadows) using remotely sensed data based on a new model that was developed in this study; (2) comparing the accuracy of different remote-sensing-based models in the GPP estimation of alpine vegetation; and (3) analysing the relationships between the key photosynthesis control factors, which are widely understood to be the functional relationship of photosynthetically active radiation (PAR) (MJ m^{-2}), the fraction of the PAR absorbed by the canopy (fPAR), and the photosynthetic efficiency term ($\varepsilon_{\perp 0}$), following the light use efficiency (LUE) approach of Monteith (1972, 1977) (e.g. Prince 1991; Goetz and Prince 1999; Heinsch et al. 2002; Turner, Ritts, et al. 2003; Turner, Urbanski, et al. 2003).

2. Methods

2.1. Study site

China possesses vast grassland resources that include alpine meadow, steppe, desert, and tundra. The total grassland area in China is approximately 400 million hectares, accounting for 41.7% of the country's land area (Ren et al. 2008). Based on temperature, the grassland regions in China fall into two categories: alpine meadow and temperate steppe (Figure 1). Alpine meadow is characterized by the presence of perennial fascicular cereal grass living in a frigid, wet, strong solar radiation, and windy environment with annual precipitation about 350–550 mm, annual average temperature below 0°C, and an altitude of approximately >3000 m. The alpine meadow in China is distributed primarily to the south and the east of the Tibetan plateau.

Our study site is located at the A'rou EC observation station (100° 27′ 52.9″ E, 38° 2′ 39.8″ N), which was constructed in July 2007 in an area of alpine meadow (Figure 1). The experimental platform is relatively flat, and the underlying surface is relatively homogeneous. The annual average temperature of the area was –0.3°C in 2009, and the annual precipitation in that year was 450.5 mm. The dominant species include Guinea grass, *Kobresia bellardii*, and *Stipa baicalensis* Roshev. The typical height of the plants is approximately 20–30 cm, but the fractional cover of vegetation is about 70–90%. The observation variables included the wind speed and direction, air temperature, precipitation, four radiation components, soil temperature and moisture profiles (measured at depths of 10, 20, 40, 80, 120, and 160 cm), and EC (measured at a height of 3.15 m). The EC measurements were commenced in June 2008, and the other measurements in July 2007 (Li et al. 2009; Wang et al. 2011).

2.2. Data

2.2.1. Climate data

The climate parameters measured in this study include air temperature, precipitation, and PAR, estimated from the downward shortwave radiation, which is equal to the difference between total radiation and longwave radiation, with a climatic coefficient of 0.43 (Wang et al. 2011). All of the related climatic parameters were measured using an automatic meteorology observation system installed at the A'rou observation station.

2.2.2. EC data

The EC data (including water vapour and CO_2 densities), latent heat flux, and sensible heat flux were collected at the A'rou station between 2008 and 2009. Water vapour density and

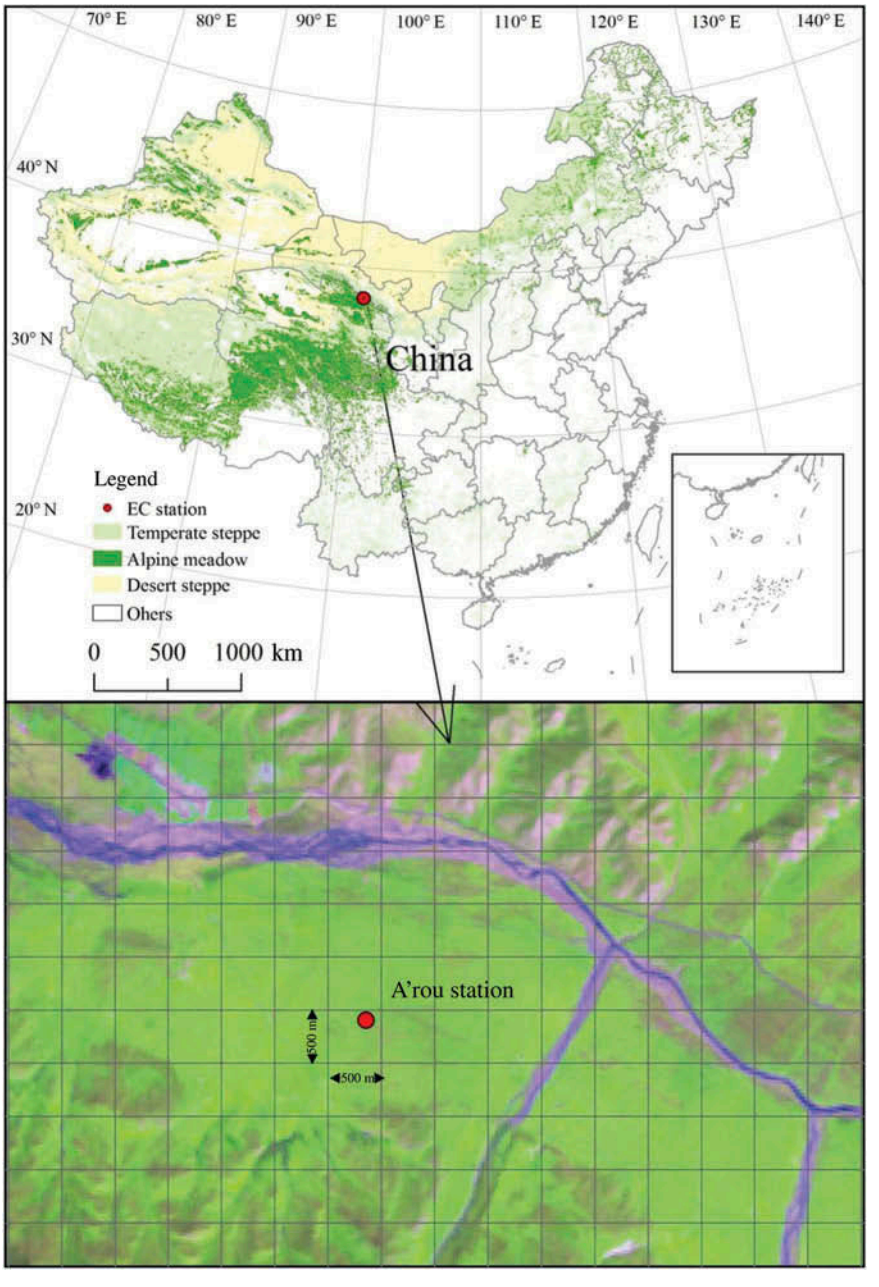

Figure 1. Distribution of grassland in China and location of A'rou station, used for EC observations.

CO_2 density were measured using an open-path, infrared gas analyser (Li-7500, LiCor Inc., USA); the sampling frequency was 10 Hz, and the energy balance ratio was approximately 87%. The latent heat flux and sensible heat flux were derived from the EC observations. The GPP can be estimated from daytime NEE, which was measured using the EC method, and the daytime ER, which was estimated using the function established by the relationship between the night-time NEE (assumed to be equal to night-time ER) and environmental factors (e.g. the air temperature, soil temperature, and soil moisture) (Equation (1)). We refer

the reader to the literature for details on data quality control and processing (Desai et al. 2008; Wang et al. 2011). The GPP is given by

$$\mathrm{GPP} = (\mathrm{NEE}) + (\mathrm{ER}), \tag{1}$$

where GPP is in units of g C m^{-2} (grammes of carbon per metre squared), NEE is the net ecosystem exchange in g C m^{-2}, and ER is the daytime ecosystem respiration, also in g C m^{-2}.

2.2.3. *Remotely sensed data*

The remotely sensed data were obtained from the moderate resolution imaging spectroradiometer (MODIS) sensor aboard the National Aeronautics and Space Administration (NASA) Terra satellite, launched in December 1999. The MODIS Land Science Team provides the user with a suite of 8 day composite products, including the 8 day surface reflectance product (MOD09A1) designed for the study of vegetation and land surfaces, with a spatial resolution of 500 m and coverage of seven spectral bands: blue (459–479 nm), green (545–565 nm), red (620–670 nm), near-infrared (841–875 and 1230–1250 nm), and shortwave infrared (1628–1652 and 2105–2155 nm).

We downloaded the 8 day surface reflectance and 8 day land-surface temperature (LST) (MOD11A2) data sets for the period January 2009 to December 2009 from the LAADS website (http://www.ladsweb.nascom.nasa.gov). Based on the geolocation information (latitude and longitude) from the CO_2 flux tower at the A'rou station, the reflectance and LST data were extracted from one MODIS pixel (500 m × 500 m) centred on the flux tower (Figure 1).

2.3. *GPP models*

One of the most widely applied methods in GPP modelling is the LUE approach, which is based on the functional convergence theory (Field 1991), which hypothesises that plants alter the canopy leaf area and harvest light according to the availability of resources as a result of evolutionary processes, in order to optimize their carbon fixation (Goetz et al. 1999). The amount of carbon fixation (photosynthesis) is generally related to environmental factors such as solar radiation, precipitation, temperature, and soil type. However, the effects of these factors on photosynthesis are still unclear. To describe the process of photosynthesis quantitatively, linear models, such as the VPM, TG, VI, and EC–LUE models, are typically employed.

2.3.1. *Vegetation photosynthesis model*

The VPM was proposed by Xiao, Hollinger, et al. (2004) and Xiao, Zhang, et al. (2004). It assumes that leaf and forest canopies are composed of photosynthetic vegetation (PAV; primarily chloroplasts) and non-photosynthetic vegetation (NPV; primarily senescent foliage, branches, and stems). The presence of NPV has a significant effect on fPAR at the canopy level. Non-photosynthetic absorption can vary in magnitude (e.g. 20–50%) depending on the species, leaf morphology, leaf age, and growth history (Hanan et al. 1998, 2002; Lambers, Chapin, and Pons 1998). Based on the conceptual partitioning of the vegetation into NPV and PAV within the leaf and canopy, VPM was defined as follows:

$$\mathrm{GPP} = \varepsilon_g \times (\mathrm{fPAR})_{\mathrm{PAV}} \times (\mathrm{PAR}), \tag{2}$$

where $\mathrm{fPAR}_{\mathrm{PAV}}$ is the fraction of the PAR absorbed by leaf chloroplasts in the canopy (Equation (3)) and ε_g is the LUE affected by the temperature, water, and leaf phenologies (see Equation (5)). The quantities on the right-hand side of Equation (2) are given by

$$\mathrm{fPAR}_{\mathrm{PAV}} = a \times (\mathrm{EVI}), \tag{3}$$

where a is a coefficient set equal to 1.0 and EVI is the enhanced vegetation index (Equation (4)):

$$\mathrm{EVI} = G\frac{\rho_{\mathrm{NIR}} - \rho_{\mathrm{red}}}{\rho_{\mathrm{NIR}} + C_1\rho_{\mathrm{red}} - C_2\rho_{\mathrm{blue}} + L}, \tag{4}$$

where ρ_{NIR}, ρ_{red}, and ρ_{blue} are the spectral reflectance in the near-infrared, red, and blue MODIS bands, respectively, and G, C_1, C_2, and L are constants with values of 2.5, 6.0, 7.5, and 1.0, respectively.

$$\varepsilon_g = \varepsilon_0 \times f(T) \times f(W) \times P_{\mathrm{scalar},} \tag{5}$$

where ε_0 is the apparent quantum yield or maximum light use efficiency; $f(T)$ (Equation (6)) is the down-regulation scalar for the effect of temperature calculated using the equation developed for the Terrestrial Ecosystem Model (TEM) (Raich et al. 1991); and $f(W)$ (Equation (7)) and P_{scalar} are the down-regulation scalars for the effects of water and leaf phenology on the light use efficiency of vegetation, respectively.

$$f(T) = \frac{(T - T_{\mathrm{min}})(T - T_{\mathrm{max}})}{(T - T_{\mathrm{min}})(T - T_{\mathrm{max}}) - (T - T_{\mathrm{opt}})^2}, \tag{6}$$

where T_{min}, T_{max}, and T_{opt} are the minimum, maximum, and optimal temperature, respectively, for photosynthetic activity. When the air temperature falls below T_{min}, T_{scalar} is set to zero. In this study, the values of T_{min}, T_{max}, and T_{opt} were set to 0°C, 35°C, and 12°C, respectively (Wang et al. 2011).

In VPM, $f(W)$ is the canopy water content calculated based on the water-sensitive vegetation index (obtained from satellite remote-sensing data) (Xiao, Hollinger, et al. 2004; Xiao, Zhang, et al. 2004). The scalar $f(W)$ is given by

$$f(W) = \frac{1 + (\mathrm{LSWI})}{1 + (\mathrm{LSWI})_{\mathrm{max}}}, \tag{7}$$

where LSWI is the water-sensitive vegetation index (see Equation (8)) and $\mathrm{LSWI}_{\mathrm{max}}$ is the maximum LSWI within the plant growing season. In Equation (7), LSWI is given by

$$\mathrm{LSWI} = \frac{\rho_{\mathrm{NIR}} - \rho_{\mathrm{SWIR}}}{\rho_{\mathrm{NIR}} + \rho_{\mathrm{SW}}}, \tag{8}$$

where ρ_{SWIR} is spectral reflectance in the shortwave MODIS bands.

P_{scalar} is used to account for the effect of leaf age on photosynthesis at the canopy level, and it depends on leaf longevity. Because the new leaves in a meadow canopy emerge

throughout a large portion of the plant growing season, P_{scalar} is set to 1.0 in this study (Li et al. 2007).

2.3.2. EC–LUE model

The EC–LUE model, developed by Yuan et al. (2007), relies on two assumptions, the first being that the fraction of absorbed PAR is a linear function of the normalized difference vegetation index (NDVI) based on a radiative transfer model (Myneni and Williams 1994). The second assumption is that the realized light use efficiency, calculated from a biome-independent invariant potential LUE, is controlled by the air temperature or soil moisture, whichever is most limiting. The EC–LUE model is driven by four variables: NDVI, PAR, air temperature, and Bowen ratio of sensible to latent heat flux. The model is defined as follows:

$$\text{GPP} = \varepsilon \times (\text{fPAR}) \times (\text{PAR}), \tag{9}$$

where fPAR is the fraction of the PAR absorbed by the vegetation canopy (see Equation (10)) and ε is the light use efficiency (see Equation (12)). The absorbed PAR fraction is given by

$$\text{fPAR} = a_0 \times (\text{NDVI}) + b_0, \tag{10}$$

where a_0 and b_0 are empirical constants. In this study, a_0 and b_0 are set to 1.24 and -0.168, respectively, following Yuan et al. (2007), and NDVI is given by the following equation:

$$\text{NDVI} = \frac{\rho_{\text{NIR}} - \rho_{\text{red}}}{\rho_{\text{NIR}} + \rho_{\text{red}}}, \tag{11}$$

where ρ_{NIR} and ρ_{red} are spectral reflectance in the near-infrared and red MODIS bands, respectively. The light use efficiency is given by

$$\varepsilon = \varepsilon_0 \times \min\{f(T), f(W)\}, \tag{12}$$

where ε_0 is the maximum light use efficiency and $f(T)$ (see Equation (6)) and $f(W)$ (see Equation (13)) are the down-regulation scalars for the respective effects of temperature and moisture on the LUE of the vegetation. The scalar $f(W)$ is given by

$$f(W) = \frac{(\text{LE})}{(\text{LE}) + (\text{HS})}, \tag{13}$$

where LE is the latent heat flux and HS is the sensible heat flux.

2.3.3. TG model

The TG model was developed by Sims et al. (2008) and was driven by EVI and LST from MODIS. In contrast to other models, the TG model was based entirely on remotely sensed data. For the data obtained from 11 EC flux towers covering a wide range of vegetation types across North America, the model performed well and provided superior predictions of GPP compared with the MODIS GPP product. The GPP was defined as

$$\text{GPP} = ((\text{scaled EVI}) \times (\text{scaled LST})) \times m, \tag{14}$$

where the scaled EVI is the difference between EVI and 0.1. The study of Sims et al. (2008) demonstrated that the GPP drops to zero at an EVI value of approximately 0.1. The quantity m is a conversion coefficient, and the scaled LST is defined as the minimum of two linear equations:

$$\text{scaled LST} = \min\left\{\frac{(\text{LST})}{20}, 2 - (0.05 \times (\text{LST}))\right\}. \tag{15}$$

This equation results in a maximum value for the scaledLST of 1.0 when LST = 30°C and a minimum value of 0.0 when LST decreases to 0°C or increases to 50°C. When the LST is greater than 50°C or less than 0°C, the scaled LST is also defined as zero.

2.3.4. *VI model*

The VI model, proposed by Wu, Han, et al. (2010), incorporates the vegetation indices for both LUE and the fraction of absorbed PAR. The model produced especially reliable proxies in maize. The VI model was defined according to Monteith's logic as follows:

$$\text{GPP} = c \times (\text{EVI})^2 \times (\text{PAR}), \tag{16}$$

where c is a conversion coefficient used in GPP estimation and the other parameters of the VI model are the same as above.

2.3.5. *Alpine vegetation model*

The LUE models, which are widely used in GPP estimation, are expressed as a function of the PAR, fPAR, maximum light use efficiency ($\varepsilon_{\perp 0}$), and environmental constraint factors (e.g. temperature and water) (Monteith 1972, 1977). The function can be partitioned into three different categories of factor, the first being fPAR, which is an 'internal' factor directly related to the primary mechanism of photosynthesis. The second category consists of environmental stresses ('external' factors), such as light stress (PAR), temperature stress, and water stress, which can considerably modify LUE (Wu, Chen, and Huang 2011). The final category is maximum light use efficiency, which depends on vegetation type and phenology.

Numerous studies on GPP have employed remotely sensed observations (e.g. use of the vegetation index) to quantify fPAR (Xiao, Hollinger, et al. 2004; Xiao, Zhang, et al. 2004; Yuan et al. 2007; Sims et al. 2008; Wu, Han, et al. 2010; Wu, Munger, et al. 2010; Wu, Chen, and Huang 2011; Wu et al. 2012). The vegetation index is a direct manifestation of the chlorophyll content within the canopy and is therefore closely related to fPAR. The factors in the first category can therefore be quantified using the vegetation index obtained from remotely sensed observations.

There are many available vegetation indices, such as NDVI (Rouse et al. 1974) and EVI (Huete et al. 1997, 2002). NDVI is the most widely applied vegetation index in evaluating optical measures of the 'greenness' of the vegetation canopy, a composite property of leaf chlorophyll, leaf area, canopy cover, and canopy architecture. However, the relationship between NDVI and chlorophyll content within the canopy is weaker in high-biomass

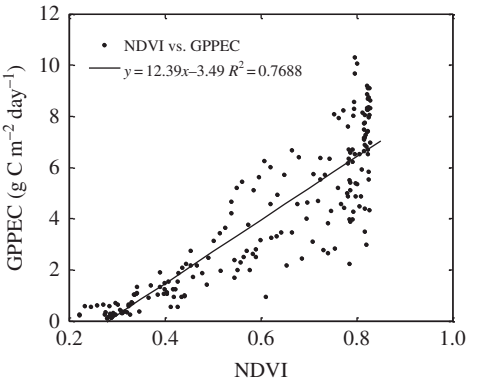

Figure 2. Relationship between NDVI and GPP–EC at A'rou station.

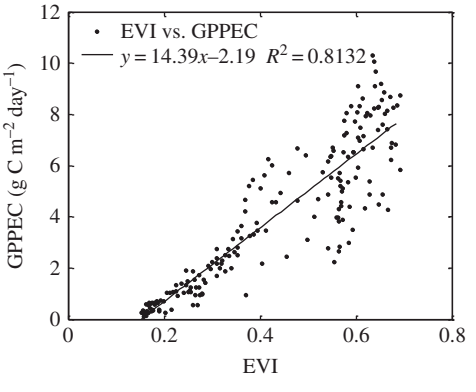

Figure 3. Relationship between EVI and GPP–EC at A'rou station.

regions due to NDVI saturation (Wang et al. 2005). In this study, for example, there is a clear saturation of NDVI above 0.8 (see Figure 2). The coefficient of determination between NDVI and GPP–EC is 0.7688. In contrast, the sensitivity of EVI improves in high-biomass environments (Jiang et al. 2008), and higher values of the coefficient of determination, $R^2 = 0.8132$, are observed in such environments (see Figure 3). EVI can therefore be adopted to explain the variance in fPAR.

Environmental stress can be quantified using environmental factors such as PAR, temperature, water availability, and soil, but the effects of these factors on photosynthesis are difficult to represent mathematically. The relationship between environmental factors and GPP is usually expressed in the form of a linear combination (see Table 1). The inclusion of a large number of environmental factors may result in large model uncertainties. In fact, there is usually only one main constraint factor in photosynthesis: for example, in alpine environments, the temperature conditions impose severe constraints on flowering phenology, reproductive success, growth, population dynamics, and phenotypic selection of quantitative traits (Billings 1987). Totland (1999) also demonstrated this phenomenon in alpine *Ranunculus acris* through experimental warming using open-top chambers (OTCs). On the other hand, temperature is closely correlated with other environmental variables, such as the vapour press deficit (VPD), PAR, and even soil moisture (Sims et al. 2008; Wu et al. 2012). The observed coefficient of determination between air temperature and GPP

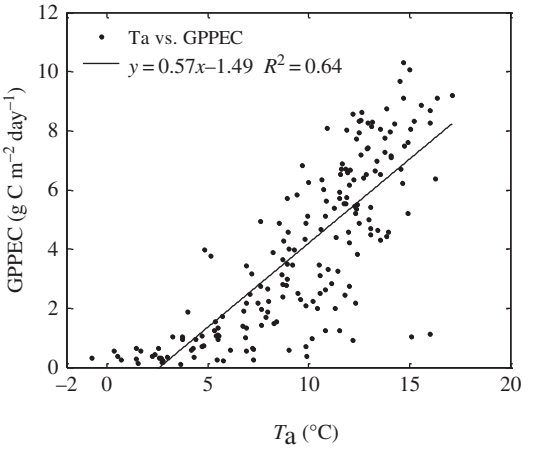

Figure 4. Relationship between T_a (air temperature) and GPP–EC at A'rou station.

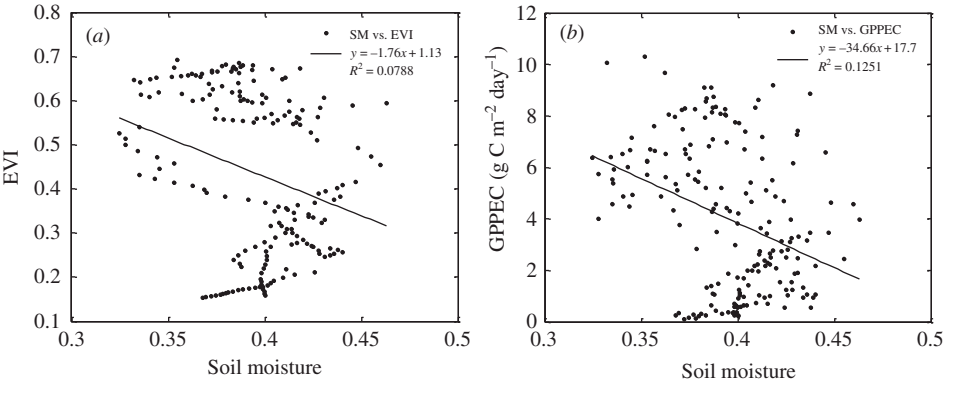

Figure 5. Relationships between soil moisture (SM) and EVI and GPP–EC at A'rou station.

obtained using the EC method (GPP–EC) was 0.64 (see Figure 4), which is higher than that between other environmental factors. In contrast, the effect of water status on GPP–EC and EVI is not clear (see Figure 5). In regard to precipitation, there is also no clear promoting effect on GPP–EC and EVI (see Figure 6). Air temperature was therefore used as the environmental stress factor in this study.

In the LUE models, the maximum light use efficiency (ε_0) must be estimated for each individual vegetation type (Wang et al. 2011; Xiao, Hollinger, et al. 2004). Furthermore, ε_0 is influenced by phenology and environmental stresses. Here, ε_0 is replaced by the fitted coefficient m (the slope) between the product of fPAR and environmental stress and GPP–EC. The slope, m, is the mean light use efficiency. The model used for GPP estimation can then be expressed as follows:

$$\mathrm{GPP} = m \times (\mathrm{fPAR}) \times E_{\mathrm{scalar}}, \tag{17}$$

where GPP is in g C m^{-2}, m is the conversion coefficient (also in g C m^{-2}) and E_{scalar} is environmental stress.

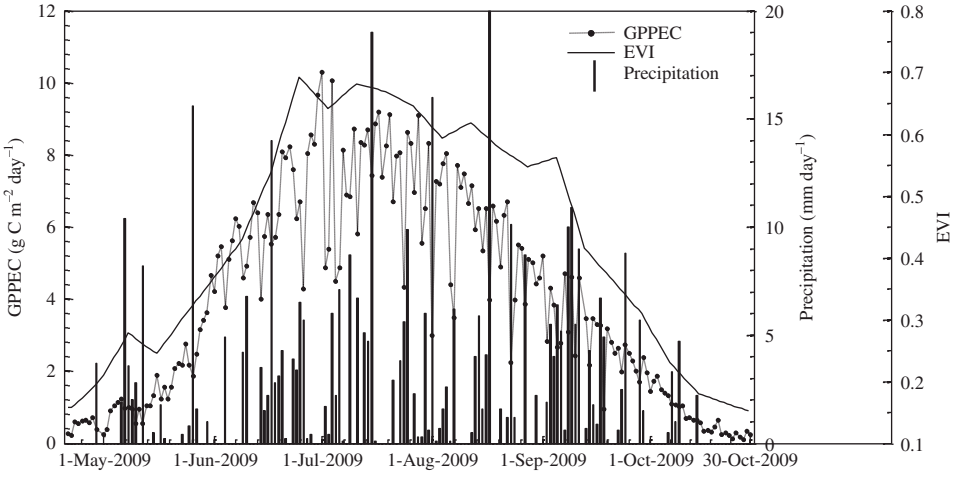

Figure 6. Growing-season dynamics of GPP, EVI, and precipitation at A'rou observation station.

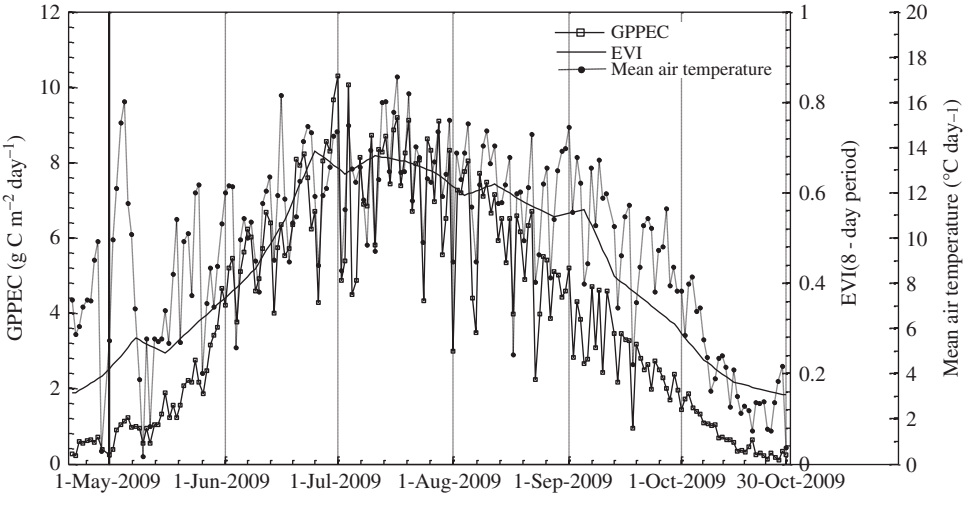

Figure 7. Growing seasonal dynamics of GPP, EVI, and daily mean air temperature at the A'rou observation station.

To substantiate Equation (17), the daily variance in GPP of alpine meadows during the growing season was accounted for in terms of EVI and air temperature (see Figure 7). The model used in this study, the alpine vegetation model (AVM), can therefore be expressed as

$$\mathrm{GPP} = m \times \mathrm{EVI}_{\mathrm{scaled}} \times T_{\mathrm{scaled}}, \tag{18}$$

where $\mathrm{EVI}_{\mathrm{scaled}}$ is given by

$$\mathrm{EVI}_{\mathrm{scaled}} = \mathrm{EVI} - \mathrm{EVI}_{\mathrm{base}}, \tag{19}$$

and T_{scaled} is the temperature stress factor, given by Equation (20). In Equation (19), EVI is given by Equation (4) and $\mathrm{EVI}_{\mathrm{base}}$ is the mean value of EVI over time when the temperature

is below 0°C (the biological temperature). The photosynthetic process is expected to cease when the temperature falls below the biological temperature. The value of EVI_{base} is taken to be 0.15. The temperature stress factor is

$$T_{scaled=}(T_a - T_{min})/(T_{max} - T_{min}), \tag{20}$$

where T_a is the daytime mean air temperature and T_{min} is the biological temperature. The maximum temperature during the alpine plant growing season is denoted by T_{max}.

3. Results

3.1. AVM estimation

It is more meaningful to measure carbon fixation during the plant growing season than to measure it year-round. In this study, GPP was therefore estimated using AVM during the growing season (from 22 April to 30 October 2009). Figure 8 shows the relationship between the product of the parameters EVI_{scaled} and T_{scaled} from the AVM and the GPP observed using the EC method (EC−GPP). The value of R^2 was 0.857. The conversion coefficient, m, was calibrated to be 19.91 g C m^{-2} with the GPP value observed at the A'rou station.

Figure 9 shows a comparison between GPP estimated using AVM (GPP–AVM) and that obtained using the EC method (GPP–EC) during the alpine plant growing season. Overall, the AVM performed very well in estimating GPP. However, GPP is underestimated by AVM during the early growing season (approximately 1 June) and at the end of the growing season (after 1 October). This discrepancy is due to our use of the mean conversion coefficient (m), which minimizes the total error.

3.2. Model comparison

Many remote-sensing-based models are used to estimate the GPP on a variety of scales ranging from local to regional and even global. However, it is very difficult to find a model

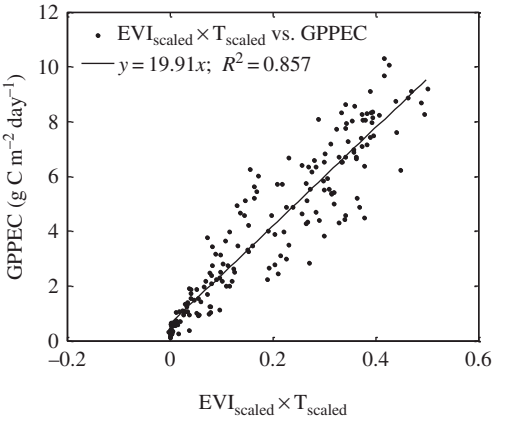

Figure 8. Relationship between $EVI_{scaled} \times T_{scaled}$ (the parameters of AVM) and GPP measured using the EC method at A'rou observation station.

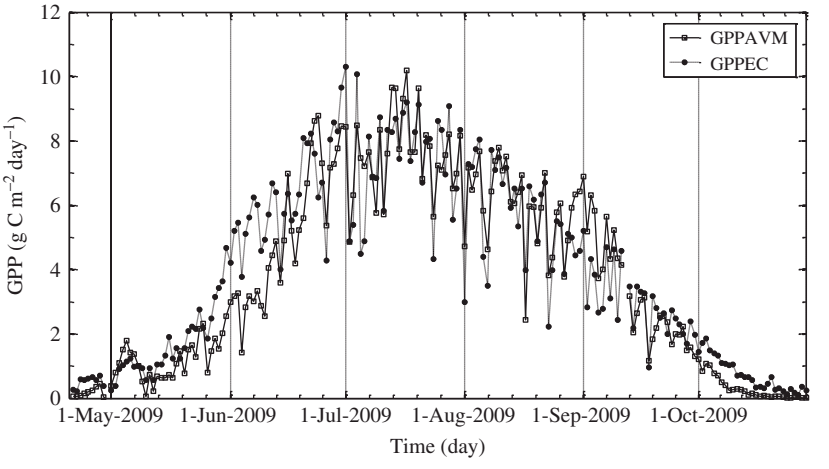

Figure 9. Comparison between GPP estimated using AVM and that obtained using the EC method during the alpine plant growing season (22 April to 30 October 2009).

capable of estimating the GPP of an entire vegetation ecosystem. Studying the suitability of models with regard to specific areas and objectives is therefore very important (Yuan et al. 2007). In this study, four models (VPM, TG, VI, and EC–LUE) were compared with AVM in terms of their accuracy in estimating the GPP of alpine vegetation. Figure 10 shows the relationship between the values estimated using the four models and GPP estimated using the EC method (GPP–EC). Overall, the four models performed well. The R^2 values for VPM, TG, VI, and EC–LUE are 0.8211, 0.8135, 0.8134, and 0.8110, respectively.

Table 2 shows that AVM estimates the GPP with a higher accuracy for alpine vegetation compared with the other four models ($R^2 = 0.857$ for AVM). The mean error, maximum deviation, and RMSE are lowest for AVM compared with the other models, thus implying that AVM may be the optimum model to reflect the daily variation in GPP over the growing season. For the aggregated estimation of GPP over the growing season, the estimate made using the TG model (about 775.79 g C m^{-2}) was closest to the observation made with EC (about 759.54 g C m^{-2}), while the estimation made with AVM was about 730.49 g C m^{-2}.

4. Discussion

Alpine plants grow in an alpine climate, which is present at high elevations and above the tree line. Most alpine plants are faced with the harsh conditions of the alpine environment, which include low temperatures, strong solar radiation, and a short growing season (Körner 2003). Explicit linear relationships are employed to simplify the complexity for a given objective, such as GPP estimation. One of the most frequently used methods for estimating GPP with remotely sensed data is the LUE approach (Sjöström et al. 2011), which links GPP to a linear combination of remotely sensed variables (e.g. EVI and NDVI) and climatic variables (e.g. PAR and temperature), as in the VPM and EC–LUE approaches.

The VPM is based on the conceptual partitioning of chlorophyll ($fPAR_{PAV}$) and non-photosynthetically active vegetation (NPV) within the canopy (Xiao, Hollinger, et al. 2004; Xiao, Zhang, et al. 2004; Xiao et al. 2005) and has been widely used in various ecosystems due to its higher accuracy in GPP estimation compared with other models (Li et al. 2007; Wang et al. 2011; Wu, Munger, et al. 2010). Li et al. (2007) demonstrated that the phase

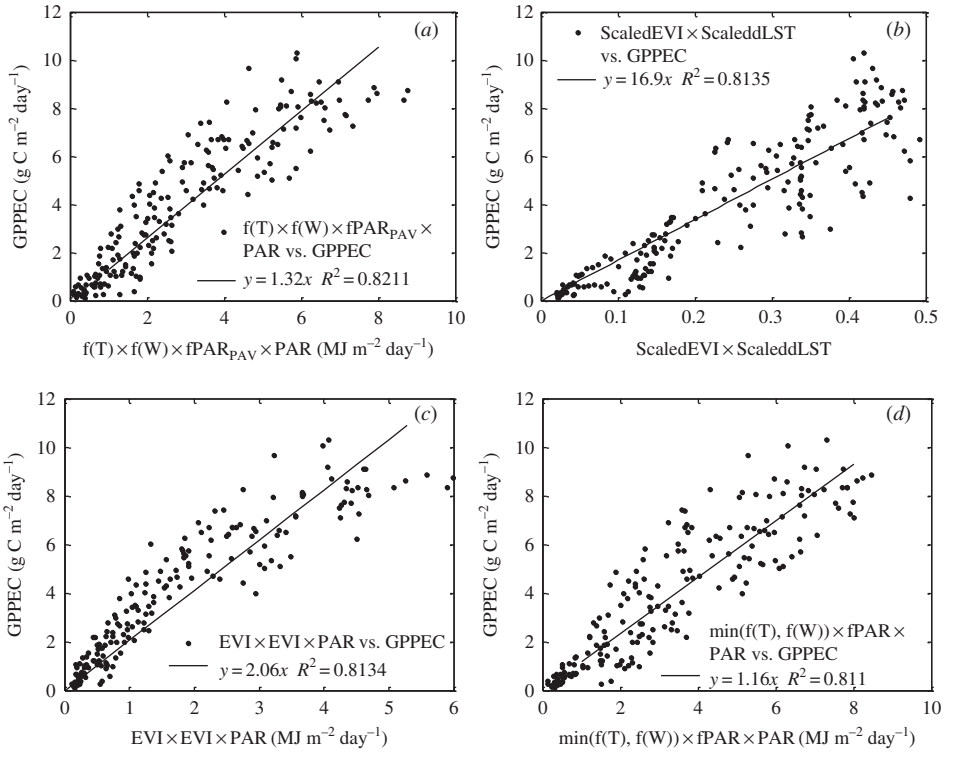

Figure 10. Coefficient calibration of the four models ((*a*) VPM, (*b*) TG, (*c*) VI, and (*d*) EC–LUE) with GPP estimated using the EC method (GPP–EC) for alpine vegetation.

Table 2. Comparison of the accuracy of the five models used for GPP estimation in alpine vegetation.

Model	Mean error (g C m^{-2} day^{-1})	Maximum deviation (g C m^{-2} day^{-1})	RMSE (g C m^{-2} day^{-1})	R^2	Aggregated growing GPP (g C m^{-2})
AVM	0.80	3.22	1.05	0.857	730.49
VPM	0.90	3.55	1.20	0.821	725.94
TG	0.92	3.81	1.22	0.814	775.79
VI	0.93	3.80	1.22	0.813	689.15
EC–LUE	0.93	3.53	1.23	0.811	742.45
GPP–EC					759.54

and magnitude of the GPP estimated using the VPM are consistent with those of the tower-based GPP for the three alpine ecosystems in the Qinghai–Tibet Plateau. The VPM uses a time series of the EVI and canopy water content $f(W)$ (Equation (7), which is calculated based on the water-sensitive vegetation index, LSWI) rather than the fraction of absorbed photosynthetically active radiation, fPAR, and the water stress factor (Xiao, Hollinger, et al. 2004; Xiao, Zhang, et al. 2004). Figure 11(*a*) shows that the coefficient of determination between $f(W)$ and the EVI is 0.9473. The scalar $f(W)$ most likely influences the accuracy of GPP estimation. The water stress factor is usually used to describe the water status of

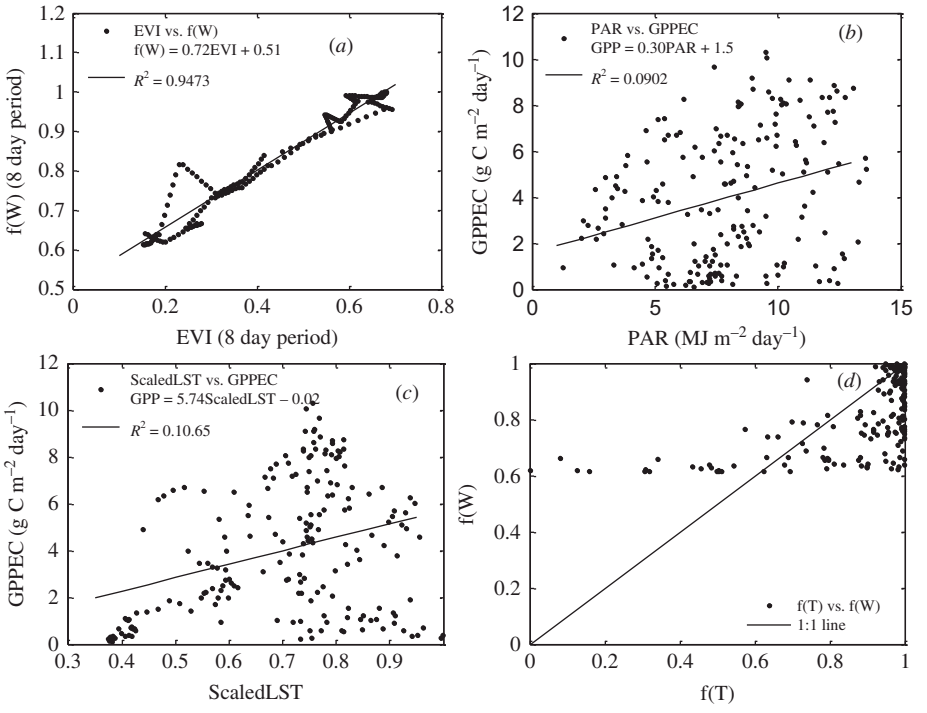

Figure 11. Relationship between the input variables of the four models (VPM, TG, VI, and EC–LUE). (*a*) and (*b*) VPM; (*b*) VI model; (*c*) TG model; (*b*) and (*d*) EC–LUE model.

the vegetation in the LUE approach (e.g. Prince 1991; Goetz and Prince 1999; Heinsch et al. 2002; Turner, Ritts, et al. 2003; Turner, Urbanski, et al. 2003). The results of the present study demonstrate that the use of the LSWI to describe the water stress factor is unreasonable. In addition, Kato et al. (2004) and Shi et al. (2006) showed that water is not a significant environmental constraint factor in alpine vegetation. In GPP estimation, it is therefore important to examine the constraining factors relevant to the specific climate and vegetation regions under study. Photosynthetically active radiation (PAR) corresponds to light in the 400–700 nm wavelength range. PAR is the light that is available for photosynthesis and that is required for plant growth. A higher PAR may, therefore, promote plant growth. However, the data obtained at the A'rou station show only a weak correlation between EC-measured GPP and PAR (Figure 11(*b*)). It is therefore likely that PAR is not a significant constraint factor in photosynthesis (Wang et al. 2011).

Regarding the EC–LUE model, it is assumed that a universal invariant potential LUE exists across all sites and biomes. The potential LUE is reduced by non-optimal temperatures or water stress. The magnitude of LUE and its relationship to the controlling factors are of crucial importance in the EC–LUE model (Yuan et al. 2007), which utilizes fPAR(NDVI) and min($f(T)$,$f(W)$) as input variables. Many studies have suggested that the quantitative relationships between vegetation indices and the GPP–EC data clearly demonstrate the improvement of EVI over NDVI in terms of the phase and magnitude of photosynthesis (Xiao, Hollinger, et al. 2004; Xiao, Zhang, et al. 2004; Xiao et al. 2005; Li et al. 2007; Wang et al. 2011; Wu, Han, et al. 2010; Wu, Munger, et al. 2010; Wu et al. 2012), especially in regions of high-density vegetation. The same conclusion was reached in this study. The aforementioned improvement is most likely due to the fact that EVI takes

more spectral information into account. In addition, we found that $\min(f(T),f(W))$ is equal to the value of $f(W)$ (Equation (13)) in most cases (Figure 11(*d*)); $f(T)$ is seldom taken into account in the EC–LUE model, which is unreasonable in alpine climatic regions.

The TG model, which uses EVI and LST (MOD11A2) as input parameters, can be used on a regional scale and even on a global scale. The model structure is similar to that of AVM. Unfortunately, LST is only an instant temperature at the time of satellite passing, and it cannot describe daily changes in temperature. Figure 11(*c*) shows that the coefficient of determination between LST and GPP is only 0.1065. However, the coefficient of determination between the air temperature observed at the meteorological station and GPP was 0.64. This result shows that the effect of LST on GPP estimation is limited by the instantaneity of LST. Another important parameter in the TG model is m (the conversion coefficient), which is calibrated using GPP data measured at EC stations (Sims et al. 2008). When this model is used to estimate GPP on a regional scale, more EC stations are needed to calibrate m. However, it is always difficult to determine this value due to the complex temporal and spatial variation of land-surface vegetation.

The VI model is defined according to Monteith logic (Wu, Han, et al. 2010). This model uses EVI and PAR as input variables, with the relationship between EVI and GPP being significant. However, the effect of the combination of these variables on GPP estimation is not clear. In addition, it is very difficult to determine the conversion coefficient, c, on a regional scale in this model.

The AVM demonstrates that GPP can be estimated at high accuracy in alpine vegetation using remotely sensed data (EVI) and climatic data (air temperature). A higher R^2 of 0.857 and lower mean error of 0.8 g C m^{-2} day^{-1} were obtained for EC-measured GPP. Regarding changes in daily GPP, Figure 9 shows a clear trend for AVM-estimated GPP to be lower than EC-measured GPP at a lower GPP range, while AVM-estimated GPP is slightly higher than EC-measured GPP near the maximum of the GPP range. This trend occurs because the mean conversion coefficient (m) was used. There is a key issue that must be considered regarding m. Grassland areas are usually interspersed with senesced grass during the early and late growing seasons, which renders a portion of photosynthetic vegetation undetectable by remote sensing, and thus produces lower EVI than its actual value. When grass approaches its maximum biomass, the vegetation coverage fraction increases, generating more shaded leaves, which cannot be detected using optical remote sensing. The influence of EVI on GPP estimation is generally different during different periods throughout the growing season (e.g. the early and middle growing seasons). The mean conversion coefficient is simply a balance between the conversion coefficients derived for these two periods. From the trends shown in Figure 9, it will also be observed that the GPP estimate using EVI in the early and late grassland growing seasons is influenced more at times corresponding to maximum biomass.

Regarding the maximum light use efficiency, ε_0, which is a key parameter in the LUE approach, incorrect estimation of ε_0 can produce a systematic bias in the simulation results (Wang et al. 2011). In this study, ε_0 was not computed in the VPM. As shown in Figure 10, VPM is simply the relationship between the product $f(T) \times f(W) \times (\mathrm{fPAR})_{\mathrm{PAV}} \times (\mathrm{PAR})$ and GPP–EC. The slope of 1.32 from the regression model was used to estimate GPP. Compared with ε_0, this slope corresponds only to the average conditions of the variables, for which the total error in the GPP estimation is minimal. However, the use of the slope underestimates GPP at low values and overestimates it at high values. This result is due to the sensitivity of EVI to senesced grass and dense canopy (which produces more shaded leaves) during certain periods. Li et al. (2007) and Wang et al. (2011) reported ε_0 values for alpine meadow of 1.83 and 1.6 g C MJ^{-1}, respectively, which are

higher than the mean conversion coefficient. GPP may, therefore, be overestimated with the ε_0 used in these studies. In contrast, the ε_0 value (1.33 g C MJ^{-1}) used by Xu et al. (2006) is very close to that used in this study. In the TG model, m was calibrated to be 16.9 g C MJ^{-1} (Figure 10(*b*)). In the VI model, c was calibrated to be 2.06 g C MJ^{-1} (Figure 10(*c*)). The maximum light use efficiency, ε_0, was not calculated in the EC–LUE model (Figure 10(*c*)). The value of 1.16 in Figure 10(*d*) for EC–LUE is simply the mean value of the light use efficiency over the entire growing season, which is close to the conversion coefficient in the VPM.

From the present study, it is evident that GPP data measured using the EC technique are required by nearly all models to accurately calibrate the conversion coefficient (m) and light use efficiency (ε), which are the basis of GPP estimation. In natural ecosystems, m and ε are determined by a wide variety of biological, biophysical, and environmental parameters (Li et al. 2007). Continuous network-based observations of CO_2 and energy fluxes over diverse ecosystems are therefore essential for the validation and calibration of models on ecosystem and regional scales (Fu et al. 2010). Although there are over 548 CO_2 eddy flux tower sites worldwide, 412 of which are active and providing copious data (http://www.fluxnet.ornl.gov/fluxnet/index.cfm), data quality and updates are still not guaranteed. Therefore, close attention should be paid to data quality evaluation and data sharing.

Remote-sensing techniques have many advantages in GPP estimation over field measurement methods and provide the potential to estimate the GPP on different scales. However, remote-sensing-based GPP estimation is a complex procedure in which many factors such as atmospheric conditions, mixed pixels, spatial heterogeneity and diversity, complex biophysical environments, insufficient EC data, calculation of ER, and data gap filling in the selected models may interactively affect GPP estimation performance. To improve this, it is critical to identify the major uncertainties during the process of developing GPP estimation models (Lu 2006; He et al. 2010). Potential solutions include (1) accurate atmospheric calibration to reduce the uncertainty caused by different atmospheric conditions; (2) the building of more EC observation stations to resolve the problems of spatial heterogeneity and diversity; (3) model validation and suitability evaluation to reduce uncertainties in GPP estimation (e.g. the suitability of AVM at other sites and in other areas still needs to be evaluated); and (4) reducing the problem of mixed pixels with the method of mixed pixel decomposition (Keshava 2003). Therefore, future studies may focus on model validation and suitability, as well as on GPP estimation and monitoring, at regional scales.

5. Conclusions

Models are important methods for researching the carbon cycle of terrestrial ecosystems. Due to different objectives and the availability of different parameters, scientists have developed many models. Taking GPP as an example, the development of a model that incorporates remotely sensed data is a common goal. However, due to ecosystem diversity and differences in climate and environment, it is always difficult to find a model that is suitable for different climate and vegetation regions.

In this study, a new method was proposed for estimating the GPP of AVM. The results showed that this model demonstrates a higher accuracy in estimating GPP compared with four other models (VPM, TG, VI, and EC–LUE). By analysing the sensitivity of the input variables in these models, we found that there is information redundancy in the input variables, which may be the reason for the lower accuracy of these models in estimating GPP compared with the AVM.

Regarding the conversion coefficient, m, in the VPM, which gives the mean conditions of the variables compared with the maximum light use efficiency, ε_0, the pattern of the VPM-estimated GPP showed underestimation at low GPP and overestimation at high GPP. These results were recorded because the sensitivity of EVI is influenced by senesced grass and dense canopy (which produces more shaded leaves) in different periods. We also found that estimates of GPP based on EVI in the early and late grassland growing seasons are affected more than near the periods of maximum biomass.

Acknowledgements

This work was supported by the 'Strategic Priority Research Programme' of the Chinese Academy of Sciences, Climate Change: Carbon Budget and Relevant Issues (Grant No. XDA05050100) and CAS Action Plan for West Development Project 'Watershed Airborne Telemetry Experimental Research (WATER)' (Grant No. KZCX2-XB2-09-03).

References

Billings, W. D. 1987. "Constraints to Plant Growth, Reproduction, and Establishment in Arctic Environments." *Arctic and Alpine Research* 19: 357–365.

Desai, A. R., A. D. Richardson, A. M. Moffat, J. Kattge, D. Y. Hollinger, A. Barr, E. Falge, A. Noormets, D. Papale, M. Reichstein, and V. J. Stauch. 2008. "Cross-Site Evaluation of Eddy Covariance GPP and RE Decomposition Techniques." *Agricultural and Forest Meteorology* 148: 821–838.

Field, C. B. 1991. "Ecological Scaling of Carbon Gain to Stress and Resource Availability." In *Integrated Responses of Plants to Stress*, edited by H. A. Mooney, S. E. Winner, and E. J. Pell, 35–65. San Diego, CA: Academic Press.

Fu, B. J., S. G. Li, X. B. Yu, P. Yang, G. R. Yu, R. G. Feng, and X. L. Zhuang. 2010. "Chinese Ecosystem Research Network: Progress and Perspectives." *Ecological Complexity* 7: 225–233.

Goetz, S. J., and S. D. Prince. 1999. "Modelling Terrestrial Carbon Exchange and Storage: Evidence and Implications of Functional Convergence in Light-Use Efficiency." *Advances in Ecological Research* 28: 57–92.

Goetz, S. J., S. D. Prince, S. N. Goward, M. M. Thawley, J. Small, and A. Johnston. 1999. "Mapping Net Primary Production and Related Biophysical Variables with Remote Sensing: Application to the Boreas Region." *Journal of Geophysical Research Atmospheres* 104: 27719–27734.

Goulden, M. L., J. W. Munger, S. M. Fan, B. C. Daube, and S. C. Wofsy. 1996a. "Measurements of Carbon Sequestration by Long-Term Eddy Covariance: Methods and a Critical Evaluation of Accuracy." *Global Change Biology* 2: 169–182.

Goulden, M. L., J. W. Munger, S. M. Fan, B. C. Daube, and S. C. Wofsy. 1996b. "Exchange of Carbon Dioxide by a Deciduous Forest: Response to Interannual Cliamte Variability." *Science* 271: 1576–1578.

Hall, F. G., J. R. Townshend, and E. T. Engman. 1995. "Status of Remote-Sensing Algorithms for Estimation of Land-Surface State Parameters." *Remote Sensing of Environment* 51: 138–156.

Hanan, N. P., G. Burba, S. Verma, J. A. Berry, A. Suyker, and E. A. Walter-Shea. 2002. "Inversion of Net Ecosystem CO_2 Flux Measurements for Estimation of Canopy PAR Absorption." *Global Change Biology* 8: 563–574.

Hanan, N., P. Kabat, A. J. Dolman, and J. A. Elbers. 1998. "Photosynthesis and Carbon Balance of a Sahelian Fallow Savanna." *Global Change Biology* 4: 523–538.

He, H. L., M. Liu, X. M. Sun, L. Zhang, Y. Q. Luo, H. M. Wang, S. J. Han, X. Q. Zhao, P. L. Shi, Y. F. Wang, Z. Ouyang, and G. R. Yu. 2010. "Uncertainty Analysis of Eddy Flux Meansurements in Typical Ecosystems of China FLUX." *Ecological Informatics* 5: 492–502.

Heinsch, F. A., M. Reeves, P. Votava, S. Kang, C. Milesi, and M. S. Zhao. 2002. *User's Guide GPP and NPP (MOD17A2/A3) Products NASA MODIS Land Algorithm, Version 2.0*. Accessed December 24, 2008. http://www.ntsg.umt.edu/modis/MOD17UsersGuide.pdf

Hilker, T., N. C. Coops, M. A. Wulder, B. T. Andrew, and R. D. Guy. 2008. "The Use of Remote Sensing in Light Use Efficiency Based Models of Gross Primary Production: A Review of Current Status and Future Requirements." *Science of the Total Environment* 404: 411–423.

Hollinger, D. Y., S. M. Goltz, E. A. Davidson, J. T. Lee, K. Tu, and H. T. Valentine. 1999. "Seasonal Patterns and Environmental Control of Carbon Dioxide and Water Vapour Exchange in an Ecotonal Boreal Forest." *Global Change Biology* 5: 891–902.

Huete, A., K. Didan, T. Miura, E. P. Rodriguez, X. Gao, and L. G. Ferreira. 2002. "Overview of the Radiometric and Biophysical Performance of the MODIS Vegetation Indices." *Remote Sensing of Environment* 83: 195–213.

Huete, A. R., H. Q. Liu, K. Batchily, and W. vanLeeuwen. 1997. "A Comparison of Vegetation Indices Global Set of TM Images for EOS-MODIS." *Remote Sensing of Environment* 59: 440–451.

Jiang, Z. Y., A. R. Huete, K. Didan, and T. Miura. 2008. "Development of a Two-Band Enhanced Vegetation Index Without a Blue Band." *Remote Sensing of Environment* 112: 3833–3845.

Kato, T., Y. H. Tang, S. Gu, X. Y. Cui, and M. Hirota. 2004. "Carbon Dioxide Exchange between the Atmosphere and an Alpine Meadow Ecosystem on the Qinghai-Tibetan Plateau, China." *Agricultural and Forest Meteorology* 124: 121–134.

Keshava, N. 2003. "A Survey of Spectral Unmixing Algorithms." *Lincoln Laboratory Journal* 14: 55–73.

Körner, C. 2003. *Alpine Plant Life: Functional Plant Ecology of High Mountain Ecosystems*. Berlin: Springer.

Lambers, H., F. S. Chapin, and T. L. Pons. 1998. *Plant Physiological Ecology*. New York: Springer-Verlag.

Landsberg, J. J., and R. H. Waring. 1997. "A Generalised Model of Forest Productivity Using Simplified Concepts of Radiation-Use Efficiency, Carbon Balance and Partitioning." *Forest Ecology Management* 95: 209–228.

Law, B. E., R. H. Waring, P. M. Anthoni, and J. D. Aber. 2000. "Measurements of Gross and Net Ecosystem Productivity and Water Vapour Exchange of a Pinus Ponderosa Ecosystem, and an Evaluation of Two Generalized Models." *Global Change Biology* 6: 155–168.

Li, X., X. W. Li, Z. Y. Li, M. G. Ma, J. Wang, Q. Xiao, and Q. Liu. 2009. "Watershed Allied Telemetry Experimental Research." *Journal of Geophysical Research* 114: D22103. doi:10.1029/2008JD011590.

Li, Z. Q., G. R. Yu, X. M. Xiao, Y. N. Li, X. Q. Zhao, C. Y. Ren, L. M. Zhang, and Y. L. Fu. 2007. "Modeling Gross Primary Production of Alpine Ecosystems in the Tibetan Plateau Using MODIS Images and Climate Data." *Remote Sensing of Environment* 107: 510–519.

Lu, D. 2006. "The Potential and Challenge of Remote Sensing-Based Biomass Estimation." *International Journal of Remote Sensing* 27: 1297–1328.

Monteith, J. L. 1972. "Solar-Radiation and Productivity in Tropical Ecosystems." *Journal of Applied Ecology* 9: 747–766.

Monteith, J. L. 1977. "Climate and Efficiency of Crop Production in Britain." *Philosophical Transactions of the Royal Society of London, Series B, Biological Sciences* 281: 277–294.

Myneni, R. B., and D. L. Williams. 1994. "On the Relationship between FAPAR and NDVI." *Remote Sensing of Environment* 49: 200–221.

Prince, S. D. 1991. "Satellite Remote-Sensing of Primary Production – Comparison of Results for Sahelian Grasslands 1981–1988." *International Journal of Remote Sensing* 31: 727–734.

Prince, S. D., and S. N. Goward. 1995. "Global Primary Production: A Remote Sensing Approach." *Journal of Biogeography* 22: 815–835.

Raich, J. W., E. B. Rastetter, J. M. Melillo, D. W. Kicklighter, P. A. Steudler, B. J. Peterson, A. L. Grace, B. Moore, and C. J. Vorosmarty. 1991. "Potential Net Primary Productivity in South-America – Application of a Global-Model." *Ecological Applications* 1: 399–429.

Ren, J. Z., Z. Z. Hu, J. Zhao, D. G. Zhang, F. J. Hou, H. L. Lin, and X. D. Mu. 2008. "A Grassland Classification Systerm and Its Application in China." *The Rangeland Journal* 30: 199–209.

Rouse, J. W., R. H. Haas, J. A. Schell, and D. W. Deering. 1974. "Monitoring Vegetation Systems in the Great Plain with ERTS." In *Proceedings, Third Earth Resources Technology Satellite-1 Symposium*, 3010–3017. Greenbelt, MD: NASA SP-351.

Running, S. W., P. E. Thornton, R. Nemani, and J. M. Glassy. 2000. "Global Terrestrial Gross and Net Primary Productivity from the Earth Observing System." In *Methods in Ecosystem Science*, edited by O. E. Sala, R. B. Jackson, and H. A. Mooney, 44–57. New York: Springer-Verlag.

Schulze, E.-D., J. Lloyd, F. M. Kelliher, C. Wirth, C. Rebmann, B. Lühker, M. Mund, A. Knohl, L. M. Milyukova, W. Schulze, W. Ziegler, A. β. Varlagin, A. F. Sogachev, R. Valentini, S. Grigoriev, O. Kolle, M. I. Panfyorov, N. Tchebakova, and N. N. Vygodskaya. 1999. "Productivity of Forests

in the Eurosiberian Boreal Region and Their Potential to Act as a Carbon Sink – A Synthesis." *Global Change Biology* 5: 703–722.

Shi, P. L., X. Z. Zhang, Z. M. Zhong, and H. Ouyang. 2006. "Diurnal and Seasonal Variability of Soil CO_2 Efflux in a Cropland Ecosystem on the Tibetan Plateau." *Agricultural and Forest Meteorology* 137: 220–233.

Sims, D. A., A. F. Rahman, V. D. Cordova, B. Z. El-Masri, D. D. Baldocchi, P. V. Bolstad, L. B. Flanagan, A. H. Goldstein, D. Y. Hollinger, L. Misson, R. K. Monson, W. C. Oechel, H. P. Schmid, S. C. Wofsy, and L. Xu. 2008. "A New Model of Gross Primary Productivity for North American Ecosystems Based Solely on the Enhanced Vegetation Index and Land Surface Temperature from MODIS." *Remote Sensing of Environment* 112: 1633–1646.

Sjöström, M., J. Ardö, A. Arneth, N. Boulain, B. Cappelaere, L. Eklundh, A. de Grandcourt, W. L. Kutsch, L. Merbold, Y. Nouvellon, R. J. Scholes, and P. Schubert. 2011. "Exploring the Potential of MODIS EVI for Modeling Gross Primary Production across African Ecosystems." *Remote Sensing of Environment* 115: 1081–1089.

Totland, Ø. 1999. "Effects of Temperature on Performance and Phenotypic Selection on Plant Traits in Alpine Ranunculus Acris." *Oecologia* 120: 242–251.

Turner, D. P., W. D. Ritts, W. B. Cohen, S. T. Gower, M. S. Zhao, S. W. Running, W. Steve, S. C. Wofsy, S. Urbanski, A. L. Dunn, and J. W. Munger. 2003. "Scaling Gross Primary Production (GPP) Over Boreal and Deciduous Forest Landscapes in Support of MODIS GPP Product Validation." *Remote Sensing of Environment* 88: 256–270.

Turner, D. P., S. Urbanski, D. Bremer, S. C. Wofsy, T. Meyers, S. T. Gower, M. Gregory. 2003. "Cross-Biome Comparison of Daily Light Use Efficiency for Gross Primary Production." *Global Chang Biology* 9: 383–395.

Veroustraete, F., H. Sabbe, and H. Eerens. 2002. "Estimation of Carbon Mass Fluxes over Europe Using the C-Fix Model and Euroflux Data." *Remote Sensing of Environment* 83: 376–399.

Wang, Q., S. Adiku, J. Tenhunen, and A. Granier. 2005. "On the Relationship of NDVI With Leaf Area Index in a Deciduous Forest Site." *Remote Sensing Environment* 94: 244–255.

Wang, X. F., M. Ma, G. Huang, F. Veroustraete, Z. Zhang, Y. Song, and J. Tan. 2011. "Vegetation Primary Production Estimation at Maize and Alpine Meadow over the Heihe River Basin, China." *International Journal of Applied Earth Observation and Geoinformation*. doi:10.1016/j.jag.2011.09.009.

Wu, C. Y., J. M. Chen, A. R. Desai, D. Y. Hollinger, M. Altaf Arain, H. A. Margolis, C. M. Gough, and R. M. Staebler. 2012. "Remote Sensing of Canopy Light Use Efficiency in Temperate and Boreal Forests of North America Using MODIS Imagery." *Remote Sensing of Environment* 118: 60–72.

Wu, C. Y., J. M. Chen, and N. Huang. 2011. "Predicting Gross Primary Production from the Enhanced Vegetation Index and Photosynthetically Active Radiation: Evaluation and Calibration." *Remote Sensing of Environment* 115: 3424–3435.

Wu, C. Y., X. Z. Han, J. S. Ni, Z. Niu, and W. Huang. 2010. "Estimation of Gross Primary Production in Wheat from in situ Measurements." *International Journal of Applied Earth Observation and Geoinformation* 12: 183–189.

Wu, C. Y., J. W. Munger, Z. Niu, and D. Kuang. 2010. "Comparison of Multiple Models for Estimating Gross Primary Production Using MODIS and Eddy Covariance Data in Harvard Forest." *Remote Sensing of Environment* 114: 2925–2939.

Xiao, J., Q. Zhuang, D. D. Baldocchi, B. E. Law, A. D. Richardson, J. Chen, R. Oren, G. Starr, A. Noormets, S. Ma, S. B. Verma, S. Wharton, S. C. Wofsy, P. V. Bolstad, S. P. Burns, D. R. Cook, P. S. Curtis, B. G. Drake, M. Falk, M. L. Fischer, D. R. Foster, L. H. Gu, J. L. Hadley, D. Y. Hollinger, G. G. Katul, M. Litvak, T. A. Martin, R. Matamala, S. McNulty, T. P. Meyers, R. K. Monson, J. W. Munger, W. C. Oechel, K. T. Paw U, H. P. Schmid, R. L. Scott, G. Sun, A. E. Suyker, and M. S. Torn. 2008. "Estimation of Net Ecosystem Carbon Exchange for the Conterminous United States by Combining MODIS and AMEriFLUX Data." *Agricultural and Forest Meteorology* 148: 1827–1847.

Xiao, J. F., Q. L. Zhuang, B. E. Law, J. Q. Chen, D. D. Baldocchi, D. R. Cook, R. Oren, A. D. Richardson, S. Wharton, S. Ma, T. A. Martin, S. B. Verma, A. E. Suyker, R. L. Scott, R. K. Monson, M. Litvak, D. Y. Hollinger, K. J. Davis, P. V. Bolstad, S. P. Burns, P. S. Curtis, B. G. Drake, M. Falk, M. L. Fischer, D. R. Foster, L. Gu, J. L. Hadley, G. G. Katul, R. Matamala, T. P. Meyers, J. W. Munger, W. C. Oechel, K. T. Paw U, H. P. Schmid, G. Starr, M. S. Torn, and S. C. Wofsy. 2010. "A Continuous Measure of Gross Primary Production for the Conterminous

United States Derived from MODIS and AMEriFLUX Data." *Remote Sensing of Environment* 114: 576–591.

Xiao, X. M., D. Hollinger, J. Aber, M. Goltz, E. A. Davidson, Q. Y. Zhang, and B. Moore III. 2004. "Satellite-Based Modeling of Gross Primary Production in an Evergreen Needleleaf Forest." *Remote Sensing of Environment* 89: 519–534.

Xiao, X. M., Q. Y. Zhang, B. Braswell, S. Urbanski, S. Boles, S. Wofsy, B. Moore III, and D. Ojima. 2004. "Modeling Gross Primary Production of Temperate Deciduous Broadleaf Forest Using Satellite Images and Climate Data." *Remote Sensing of Environment* 91: 256–270.

Xiao, X. M., Q. Y. Zhang, S. Saleska, L. Hutyra, P. De Camargo, S. Wofsy, S. Frolking, S. Boles, M. Keller, and B. Moore III. 2005. "Satellite-Based Modeling of Gross Primary Production in a Seasonally Moist Tropical Evergreen Forest." *Remote Sensing of Environment* 94: 105–122.

Xu, L. L., X. Z. Zhang, P. L. Shi, and G. R. Yu. 2006. "Response of Canopy Quantum Yield of Alpine Meadow to Temperature under Low Atmospheric Pressure on Tibetan Plateau." *Science in China D: Earth Sciences* 49 (Supp. II): 219–225.

Yu, G. R., Y. L. Fu, X. M. Sun, X. F. Wen, and L. M. Zhang. 2006. "Recent Progress and Future Directions of China FLUX. Science in China Series D." *Earth Sciences* 49: 1–23.

Yu, G. R., X. F. Wen, B. D. Tanner, X. M. Sun, X. H. Lee, and J. Y. Chen. 2006. "Overview of China FLUX and Evaluation of Its Eddy Covariance Measurement." *Agricultural and Forest Meteorology* 137: 125–137.

Yu, G. R., L. M. Zhang, X. M. Sun, Y. L. Fu, X. F. Wen, Q. F. Wang, S. G. Li, C. Y. Ren, X. Song, Y. F. Liu, S. J. Han, and J. H. Yan. 2008. "Environmental Controls over Carbon Exchange of Three Forest Ecosystems in Eastern China." *Global Change Biology* 14: 2555–2571.

Yuan, W., S. Liu, G. Zhou, G. Zhou, L. L. Tieszen, D. Baldocchi, C. Bernhofer, H. Gholz, A. H. Goldstein, M. L. Goulden, D. Y. Hollinger, Y. M. Hu, B. E. Law, P. C. Stoy, T. Vesala, and S. C. Wofsy. 2007. "Deriving a Light Use Efficiency Model from Eddy Covariance Flux Data for Predicting Daily Gross Primary Production Across Biomes." *Agricultural and Forest Meteorology* 143: 189–207.